AJNR

Imaging Features with Histopathologic Correlation of CNS High-Grade Neuroepithelial Tumors with a *BCOR* Internal Tandem Duplication

L. Cardoen, A. Tauziède-Espariat, V. Dangouloff-Ros, S. Moalla, N. Nicolas, C.-J. Roux, Y. Bouchoucha, F. Bourdeaut, K. Beccaria, S. Bolle, G. Pierron, C. Dufour, F. Doz, N. Boddaert and H.J. Brisse

AJNR Am J Neuroradiol 2022, 43 (1) 151-156
doi: https://doi.org/10.3174/ajnr.A7367
http://www.ajnr.org/content/43/1/151

Imaging Features with Histopathologic Correlation of CNS High-Grade Neuroepithelial Tumors with a *BCOR* Internal Tandem Duplication

L. Cardoen, A. Tauziède-Espariat, V. Dangouloff-Ros, S. Moalla, N. Nicolas, C.-J. Roux, Y. Bouchoucha, F. Bourdeaut, K. Beccaria, S. Bolle, G. Pierron, C. Dufour, F. Doz, N. Boddaert, and H.J. Brisse

ABSTRACT

BACKGROUND AND PURPOSE: A new brain tumor entity occurring in early childhood characterized by a somatic *BCL6* corepressor gene internal tandem duplication was recently described. The aim of this study was to describe the radiologic pattern of these tumors and correlate this pattern with histopathologic findings.

MATERIALS AND METHODS: This retrospective, noninterventional study included 10 children diagnosed with a CNS tumor, either by ribonucleic acid–sequencing analysis or deoxyribonucleic acid methylation analysis. Clinical, radiologic, and histopathologic data were collected. A neuropathologist reviewed 9 tumor samples. Preoperative images were analyzed in consensus by 7 pediatric radiologists.

RESULTS: All tumors were relatively large (range, 4.7–9.2 cm) intra-axial peripheral masses with well-defined borders and no peritumoral edema. All tumors showed mild and heterogeneous enhancement and marked restriction on DWI of the solid portions. Perfusion imaging showed a relatively lower CBF in the tumor than in the adjacent normal parenchyma. Nine of 10 tumors showed areas of necrosis, with the presence of hemorrhage in 8/10 and calcifications in 4/7. Large intratumoral macroscopic veins were observed in 9/10 patients. No intracranial or spinal leptomeningeal dissemination was noted at diagnosis.

CONCLUSIONS: CNS tumors with a *BCL6* corepressor gene internal tandem duplication present as large intra-axial peripheral masses with well-defined borders, no edema, restricted diffusion, weak contrast enhancement, frequent central necrosis, hemorrhage and calcifications, intratumoral veins, and no leptomeningeal dissemination at the time of diagnosis. Knowledge of these imaging characteristics may aid in histologic, genomic, and molecular profiling of brain tumors in young children.

ABBREVIATION: ITD = internal tandem duplication

Recently, a new group of CNS tumors characterized by a genetic *BCL6* corepressor (*BCOR*) alteration and distinct histopathologic and clinical features was identified.[1] CNS tumors with an internal tandem duplication (ITD) of the *BCOR* gene, formerly included in the group of primitive neuroectodermal tumors of the CNS, form a specific molecular entity.[2]

To date, 50 cases have been reported,[1,3-13] with mainly a genomic and histopathologic description. Only 2 publications included a few MR images[6,12] but no detailed discussion of the CT and MR imaging features.

The aim of our study was to report a series of CNS tumors with a proved somatic *BCOR* ITD, to describe their radiologic patterns on CT and MR imaging, and to correlate these patterns with the histopathologic findings.

MATERIALS AND METHODS

This retrospective noninterventional study was approved by the institutional review board of the Institut Curie, with a waiver of the requirement for patient consent.

Patients

Ten children were diagnosed with a CNS tumor with a *BCOR* ITD during 2010–2019 in France, either by ribonucleic acid–sequencing

Received July 15, 2021; accepted after revision September 27.

From the Imaging Department (L.C., N.N., H.J.B.), SIREDO Oncology Center Care, Innovation and Research for Children, Adolescents and Young Adults with Cancer (Y.B., F.B., F.D.), and Department of Biopathology and Genetics (G.P.), Institut Curie, Paris, France; Department of Neuropathology (A.T.-E.), Centre Hospitalier Sainte Anne, Paris, France; Department of Neurosurgery (K.B.) and Pediatric Radiology Department (V.D.-R., C.-J.R., N.B.), Assistance Publique–Hôpitaux de Paris, Hôpital Universitaire Necker-Enfants Malades, Paris, France; Institut Imagine (V.D.-R., N.B.), Université de Paris, Unité Médicale de Recherche (UMR) 1163, Paris, France; Departments of Radiology (S.M.), Radiation Oncology (S.B.), and Paediatric and Adolescent Oncology (C.D.), Gustave Roussy, Villejuif, France; Université de Paris (V.D.-R., K.B., F.D., N.B.), Institut National de la Santé et de la Recherche Médicale, ERL UA10, Paris, France; and Université Paris Saclay (H.J.B.), Institut National de la Santé et de la Recherche Médicale, LITO U1288, Orsay, France.

Please address correspondence to Liesbeth Cardoen, MD, Institut Curie, 26, rue d'Ulm, Paris 75248, France; e-mail: liesbeth.cardoen@curie.fr

Indicates article with online supplemental data.

http://dx.doi.org/10.3174/ajnr.A7367

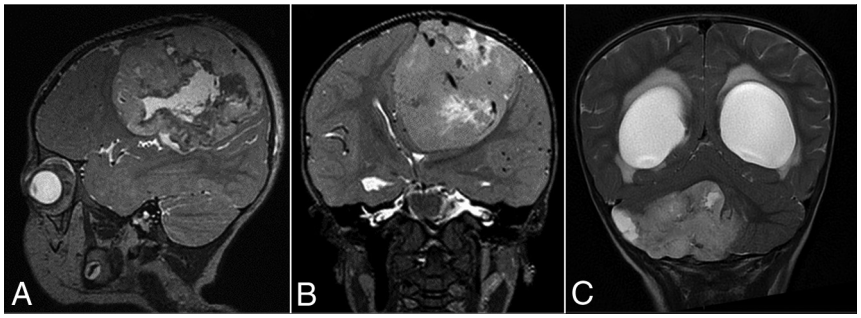

FIG 1. T2-weighted MR images showing large masses located supratentorially (*A* and *B*) and infratentorially (*C*).

analysis performed at 2 expert centers (Institut Curie in Paris and Center Léon Bérard in Lyon, France) or by deoxyribonucleic acid methylation analysis in the Neuropathology Department of Sainte-Anne Hospital (Paris, France) using the Deutsches Krebsforschungszentrum/Heidelberg University classifier.[14] Medical records were searched retrospectively for the collection of clinical, radiologic, and histopathologic data.

One patient in the cohort (patient 6) was previously included in the article by Appay et al.[5]

Histopathology

All tumor samples were evaluated by an experienced neuropathologist (9/10 were reviewed by A.T.-E., and the histopathologic findings from 1 tumor sample were previously published[5]) using hematoxylin phloxine saffron staining. For each tumor sample, we analyzed the following criteria: cellular density, the presence of necrosis, calcifications, hemorrhagic modifications, the density of the vascular network, and the presence of microvascular proliferation. The infiltrative or well-circumscribed growth pattern of the tumors was evaluated using an antibody against neurofilament (1:100, clone NF70; Dako). The density of the vascular network was evaluated using a CD34 antibody (1:40, clone QBEnd10; Dako).

Imaging

Both MR imaging and CT scans of the brain were available for 5 patients, MR images only were available for 4 patients, and only CT scans were available for 1 patient. MR imaging of the spinal axis was available for 6 patients.

MR imaging was performed at different institutions. At a minimum, the acquired sequences were T1-weighted, T2-weighted, DWI, and T1-weighted imaging after contrast media injection. The MR imaging investigation of 1 patient included unenhanced perfusion imaging a with 3D pseudocontinuous arterial spin-labeling sequence, and another patient had a dynamic susceptibility contrast-enhanced perfusion-weighted (T2*) sequence. CT images before and after iodine contrast media injection were also reviewed. The presence of calcifications was assessed either by unenhanced CT or the comparison of phase and magnitude images from SWI when available.

The preoperative images of each patient were analyzed by 7 pediatric radiologists (L.C., H.J.B., N.N., N.B., V.D.-R., C.-J.R., and S.M.), with 6, 25, 4, 20, 9, 8, and 5 years' experience, respectively, who came to a consensus regarding the findings. Images were qualitatively analyzed using the viewer of the PACS of the Institut Curie.

RESULTS

Clinical Findings

The study population included 7 girls and 3 boys. The age of the patients ranged from 1.2 years to 7.6 years with a median age of 1.8 years. The clinical symptoms at diagnosis were mainly intracranial pressure and ataxia and hemiparesis and convulsions.

Histopathologic Findings

All tumors were densely cellular and well-circumscribed from the normal brain parenchyma, as confirmed by neurofilament staining. Hemorrhagic modifications were present in 6/9 tumors. A dense branching capillary network was present in all tumors, confirmed by CD34 immunostaining, with hyalinized fibrous vessels in 2 tumors. However, no large vessels, including veins, were observed in any tumors. Only 2 tumors presented with calcifications in the viable portion of the tumor. Palisading, geographic, and calcified necrosis was observed in 6/9 tumors. Microvascular proliferation was present in only 1 tumor. Leptomeningeal involvement in 1 tumor was confirmed histopathologically.

Imaging Features

Findings are reported in the Online Supplemental Data.

All tumors were relatively large, well-defined intra-axial masses, with the largest median diameter being 6 cm (range, 4.7–9.2 cm) and the median volume being 48 cm^3 (range, 26–208 cm^3) (Fig 1).

Five tumors were located supratentorially, 2 in the frontal lobe, 2 in the temporal lobe, and 1 centered on the fornix. The 5 tumors situated infratentorially were all cerebellar hemisphere masses. Nine of 10 tumors were localized peripherally—ie, they abutted the overlying dura but showed no radiologic signs of dural invasion.

On MR imaging, tumors showed a low signal intensity on T1-weighted images and a signal intensity on T2-weighted images slightly higher than that of the normal gray matter. Nine of 10 tumors showed areas of necrosis with the presence of hemorrhage in 8/10 and calcifications in 4/7 at the border of the necrotic area and the solid portions of the tumor (Figs 2 and 3). On CT, tumor density was measured between 26 and 38 HU (versus 35 HU for normal cortical gray matter). No vasogenic edema in the surrounding white matter was observed for any tumor.

All tumors demonstrated a restriction of diffusion, with ADC values varying between 0.5 and 0.9 $\times$ $10^{-3}$$mm^2$/s (Fig 4) (the ADC values measured in the normal cortical gray matter of our patients ranged between 0.8 and 1.0 $\times$ $10^{-3}$$mm^2$/s.

Large intratumoral macroscopic vessels connected to cortical veins were observed in 9/10 patients. All tumors showed mild and heterogeneous enhancement of the solid portion on MR imaging or CT (Fig 5). For patient n° 4, the CBF measured with arterial spin-labeling was 37 mL/min/100g and the relative CBF compared

with that of the contralateral cortical gray matter was 0.52. By T2* perfusion-weighted MR imaging, the relative CBV was 1.91 and the relative CBF was 0.87 for patient n° 6.

No intracranial or spinal leptomeningeal dissemination was noted at diagnosis.

Treatment

All patients underwent an initial operation, with macroscopic complete resection in 9/10 patients. Seven patients received adjuvant chemotherapy. Eight patients received adjuvant external radiation therapy on the tumor bed, and 6 received additional craniospinal radiation therapy.

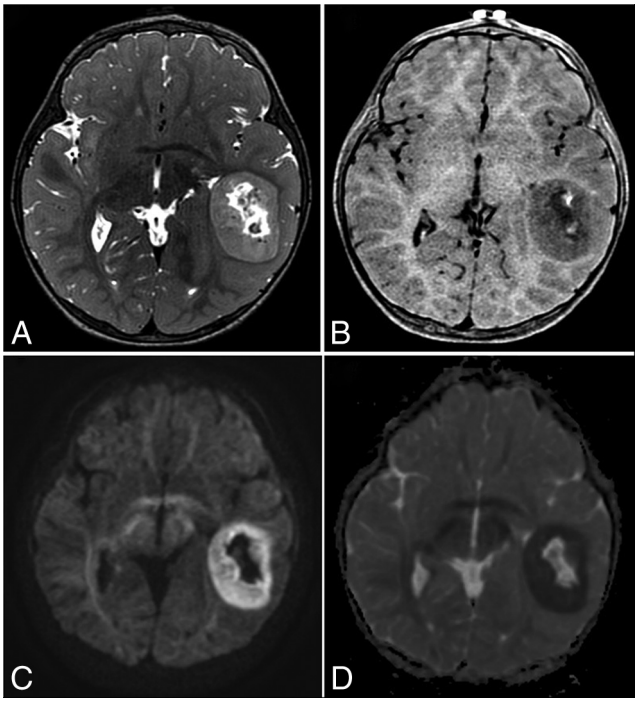

FIG 2. Characteristic MR imaging features of CNS tumors with a *BCOR* ITD. *A*, Axial T2-weighted image shows a well-defined mass, central necrosis, and no surrounding edema. *B*, Axial contrast-enhanced T1-weighted image shows poor enhancement after contrast medium administration. Axial DWI (*C*) and ADC map (*D*) show restricted diffusion of the solid portions of the tumor.

Clinical/Patient Outcomes

Six patients died of their disease within 9–71 months of diagnosis (patient n° 1, 2, 3, 7, 8, 9). Three patients still have a complete response: Two patients (n° 5 and 6) had an initial complete response 19 and 51 months from diagnosis, and 1 patient (n° 4) had a second complete response 69 months from diagnosis. One patient is still being treated (n° 10).

DISCUSSION

CNS tumors with a *BCOR* ITD are a new tumor entity occurring in early childhood and are characterized by a specific genetic *BCOR* alteration and distinct histopathologic features. To the best of our knowledge, this series, though small, is the largest for which a detailed radiologic description correlated with the histopathologic characteristics is presented.

Genomic profiling of these tumors revealed a somatic ITD in the region of exon 15 of the *BCOR* gene. Somatic alterations in *BCOR* have been identified as recurrent genetic drivers in a wide spectrum of human tumor types. The same type of duplication in *BCOR* has been described in clear cell sarcoma of the kidney[15-17] and in a subset of soft-tissue undifferentiated, primitive myxoid mesenchymal tumors of infancy.[18,19]

CNS tumors with a *BCOR* ITD are compact tumors with predominantly solid growth, characterized by a combination of spindle and oval cells. The histopathologic analysis demonstrates cytologic and immunohistochemical evidence of neuroepithelial differentiation. Histologic features such as fibrillary processes, characteristics of glial differentiation, perivascular pseudorosettes, and palisading necrosis have been reported. In contrast to ependymomas however, CNS tumors with a *BCOR* ITD exhibit sparse-to-no expression of glial fibrillary acidic protein or S-100. The typical embryonal morphology as seen in embryonal tumors and evident neuronal differentiation is not observed.[1]

According to our study cohort, in CT and MR imaging, CNS tumors with a *BCOR* ITD present as relatively large intra-axial and peripheral masses with well-defined borders without peripheral edema, confirmed by pathology and in agreement with the few cases previously described.[3,6,8,12,13] An equal distribution between supratentorial and infratentorial locations was observed in our cohort, but a slight predominance of an infratentorial location has been reported in the literature.[3-9,11-13] CNS tumors with a *BCOR* ITD are located mainly in the cerebral or cerebellar hemispheres. In accordance with Ferris et al,[12] who reported that most tumors abutted the overlying dura without definite invasion, we also observed contact with the dura mater in 9 of 10 patients. This finding was not clearly described in the few previously published cases; however, this pattern was retrospectively visible in the published images.[3-5,8,13] Despite the peripheral location, no dural tail sign or thickening of the dura mater, suggesting leptomeningeal dissemination, was observed at the time of diagnosis, as previously described.[7,8,12] One patient had focal leptomeningeal

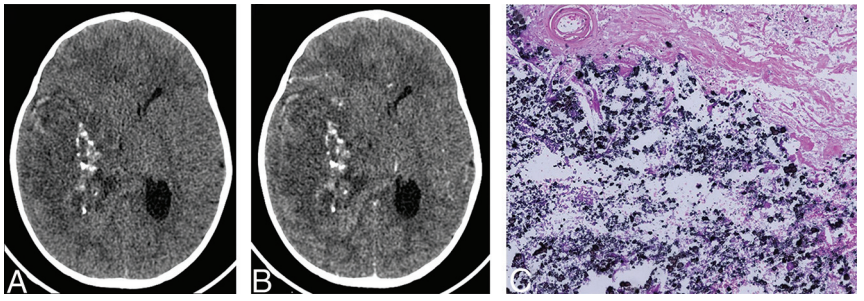

FIG 3. Axial CT images before (*A*) and after (*B*) contrast medium administration. The tumor is hypo to isodense relative to the cortex, and it exhibits weak-to-mild contrast enhancement. Intralesional calcifications are well-visualized. *C*, Visualization of several calcifications (*black stained*) (hematoxylin phloxine saffron, original magnification ×100).

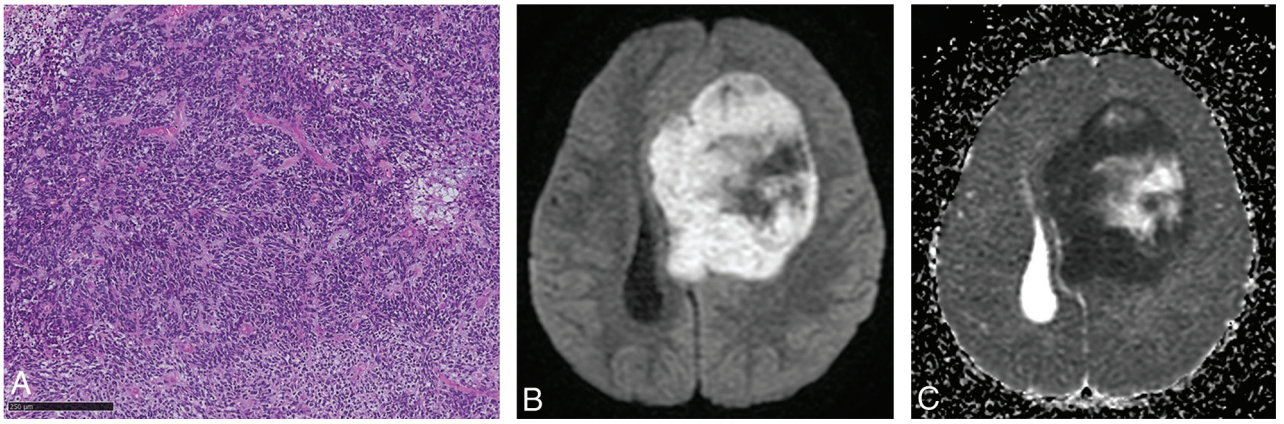

FIG 4. *A*, High cellular density of the tumor with numerous nuclei, densely packed (hematoxylin phloxine saffron, original magnification ×100). *Black scale bar* represents 250 μm. Note the corresponding diffusion-weighted image (*B*) with ADC mapping (*C*).

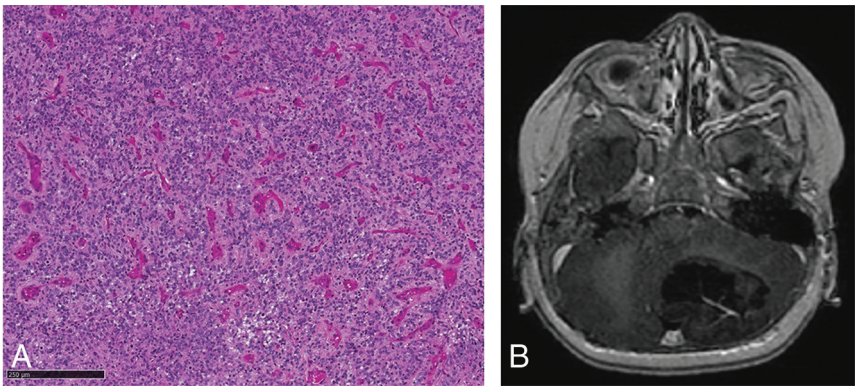

FIG 5. *A*, Rich delicate thin-walled vessels without microvascular proliferation (hematoxylin phloxine saffron, original magnification ×100). *Black scale bar* represents 250 μm. *B*, Corresponding contrast-enhanced T1-weighted MR image shows weak contrast uptake.

metastases identified on histopathologic examination, which were not visible on imaging probably because of the low sensitivity of the CT scan (no MR image was available). These imaging findings, consistent with the histopathologic findings, suggest an intraparenchymal origin of these tumors and not a mesenchymal origin as is the case of *BCOR* ITD tumors occurring in the kidney and soft tissue.

The solid portions of the tumor were hypointense on T1-weighted images and slightly hyperintense on T2-weighted images, and they showed a marked restriction on DWI related to their high cellular density. Ferris et al[12] described a more heterogeneous T2 signal, which varied from isointense to hyperintense compared with the adjacent brain. To our knowledge, the CT density of CNS tumors with a *BCOR* ITD has never been reported.

Our histopathologic results showed a high microvascular density but no microvascular proliferation for all tumors. In agreement with earlier imaging reports,[5,6,12] we also observed weak contrast enhancement of these tumors. Indeed, it has been previously reported that contrast enhancement is not a criterion for high-grade neoplasms in children.[20,21] Perfusion imaging was available in only 2 patients but demonstrated relatively low-to-intermediate CBF values compared with the adjacent normal parenchyma. This finding has not yet been reported in the radiologic literature, surprising because CBF was reported to be correlated with tumor microvascular density and histologic grade in children.[21] However, low CBF values were also reported for other high-grade tumors such as embryonal tumors with multilayered rosettes.[20] The relative CBV value for 1 patient was elevated; hence, the low CBF could be related to a long MTT in capillary vessels. These findings should be confirmed in a larger patient sample. We suggest that the relationship between perfusion and tumor neovascularization is probably multifactorial and not solely determined by vessel density and vessel wall structure.

We did not observe vasogenic edema within the surrounding white matter. This relatively uncommon finding for high-grade CNS tumors was also noted by Ferris et al[12] and Bremer et al[13] and was retrospectively visible on the available images from other published cases.[3,5,6,8] Almost all studies described areas of necrosis and blood products.[6,8,12,13] We observed calcifications located at the border of the central necrotic area and the solid peripheral portion of the tumor, a finding that had not been previously described. A possible explanation is that calcifications are more easily seen on CT and the available imaging in preceding studies was mainly MR images. Large central veins located within the mass were a feature observed in almost all our patients and have not been described to date. This finding was not correlated with pathology, probably because of tumor sampling bias.

Knowledge of these imaging features might help in the consideration of this type of tumor when facing the initial diagnosis of a brain tumor in a young child. A possible differential diagnosis is an embryonal tumor with multilayered rosettes, a rare malignant embryonal tumor occurring in the same age group that shares some features with CNS tumors with a *BCOR* ITD. Embryonal tumors with multilayered rosettes are also large tumors with

frequent calcifications, little-to-no edema, absent or weak contrast enhancement, intratumoral veins, restricted diffusion, and low CBF values in arterial spin-labeling.[20] However, in contrast to CNS tumors with a *BCOR* ITD, embryonal tumors with multilayered rosettes do not exhibit frequent central necrosis.

Primary atypical teratoid/rhabdoid tumors are another type of rare, highly malignant embryonal tumor occurring in young children. Imaging features that may distinguish them from CNS tumors with a *BCOR* ITD are the presence of peripheral cystic components, some mild-to-moderate edema, a marked enhancement of the solid portions of the tumor, and tumor dissemination within the CNS at the time of diagnosis.[22-26]

Medulloblastomas typically occur in mid-childhood (5–7 years). Most medulloblastomas occurring in early childhood belong to the sonic hedgehog group, group 3 or 4. Group 3 and 4 medulloblastomas arise from the midline (vermis and fourth ventricle) and frequently show early metastasis.[27,28] Sonic hedgehog medulloblastomas in infants with desmoplastic and nodular histologic features are located in the cerebellar hemispheres and arise from the cerebellar cortex. Sonic hedgehog medulloblastomas with extensive nodularity display a more diffuse nodular grape-like pattern on MR images than CNS tumors with a *BCOR* ITD. Moreover, sonic hedgehog medulloblastomas commonly display very strong postcontrast enhancement, which is thought to be due to leptomeningeal desmoplasia.[29]

Most ependymomas have an infratentorial intraventricular location with an extension of the tumor through the foramen of the fourth ventricle. Supratentorial ependymomas have an intraparenchymal location. They tend to be more T2-hyperintense than CNS tumors with a *BCOR* ITD, with the presence of large cysts, avid heterogeneous enhancement, and intermediate diffusion restriction.[30] Low-grade gliomas have highly variable imaging features. They generally show an increased diffusivity on ADC maps. High-grade gliomas have more irregular and infiltrative margins and exhibit peritumoral edema and more contrast uptake than CNS tumors with a *BCOR* ITD.[27]

CNS tumors with a *BCOR* ITD are aggressive tumors that require close clinical and radiologic monitoring. Despite intensive treatment, CNS tumors with a *BCOR* ITD are associated with early local recurrence and a poor outcome. Different treatments have been attempted, such as total surgical excision, focal or craniospinal radiation therapy, chemotherapy (including carboplatin, cisplatin, etoposide, cyclophosphamide, procarbazine, and temozolomide), bevacizumab, intrathecal chemotherapy (methotrexate and topotecan), and high-dose chemotherapy with autologous stem cell support. New treatment strategies are being investigated.[4,7,10]

Due to the rarity of this disease, the relatively small number of CNS tumors with a *BCOR* ITD is a limitation of our study. Because the images were evaluated retrospectively and imaging was performed at different centers, our data also show a certain degree of heterogeneity, and notably, CT and functional imaging were not available for all patients, especially perfusion imaging.

CONCLUSIONS

We described the imaging features of 10 confirmed CNS tumors with a *BCOR* ITD, and we correlated these features with the clinical and histopathologic findings. CNS tumors with a *BCOR* ITD present as large peripheral intra-axial masses with well-defined borders, no edema, restricted diffusion, weak contrast enhancement, frequent central necrosis, hemorrhage and calcifications, intratumoral veins, and no leptomeningeal dissemination at the time of diagnosis. Knowledge of these characteristics may aid in the histologic, genomic, and molecular profiling of brain tumors in young children.

ACKNOWLEDGMENTS

We thank Dr Marie Simbozel for assistance with data collection.

Disclosure forms provided by the authors are available with the full text and PDF of this article at www.ajnr.org.

REFERENCES

1. Sturm D, Orr BA, Toprak UH, et al. **New brain tumor entities emerge from molecular classification of CNS-PNETs.** *Cell* 2016;164:1060–72 CrossRef Medline
2. Louis DN, Perry A, Wesseling P, et al. **The 2021 WHO Classification of Tumors of the Central Nervous System: a summary.** *Neuro Oncol* 2021; 23:1231–51 CrossRef Medline
3. Kline CN, Joseph NM, Grenert JP, et al. **Targeted next-generation sequencing of pediatric neuro-oncology patients improves diagnosis, identifies pathogenic germline mutations, and directs targeted therapy.** *Neuro Oncol* 2017;19:699–709 CrossRef Medline
4. Paret C, Theruvath J, Russo A, et al. **Activation of the basal cell carcinoma pathway in a patient with CNS HGNET-BCOR diagnosis: consequences for personalized targeted therapy.** *Oncotarget* 2016;7:83378–91 CrossRef Medline
5. Appay R, Macagno N, Padovani L, et al. **HGNET-BCOR tumors of the cerebellum.** *Am J Surg Pathol* 2017;41:1254–60 CrossRef Medline
6. Yoshida Y, Nobusawa S, Nakata S, et al. **CNS high-grade neuroepithelial tumor with BCOR internal tandem duplication: a comparison with its counterparts in the kidney and soft tissue.** *Brain Pathol* 2018;28:710–20 CrossRef Medline
7. Paret C, Russo A, Otto H, et al. **Personalized therapy: CNS HGNET-BCOR responsiveness to arsenic trioxide combined with radiotherapy.** *Oncotarget* 2017;8:114210–25 CrossRef Medline
8. Al-Battashi A, Al Hajri Z, Perry A, et al. **A cerebellar high-grade neuroepithelial tumour with BCOR alteration in a five-year-old child.** *Sultan Qaboos Univ Med J* 2019;19:153–56 CrossRef Medline
9. Kirkman M, Pickles J, Fairchild A, et al. **Early wound site seeding in a patient with central nervous system high-grade neuroepithelial tumor with BCOR alteration.** *World Neurosurg* 2018;116:279–84 CrossRef Medline
10. Vewinger N, Huprich S, Seidmann L, et al. **IGF1R is a potential new therapeutic target for HGNET-BCOR brain tumor patients.** *Int J Mol Sci* 2019;20:3027 CrossRef Medline
11. Łastowska M, Trubicka J, Sobocińska A, et al. **Molecular identification of CNS NB-FOXR2, CNS EFT-CIC, CNS HGNET-MN1 and CNS HGNET-BCOR pediatric brain tumors using tumor-specific signature genes.** *Acta Neuropathol Commun* 2020;8:105 CrossRef Medline
12. Ferris S, Velazquez Vega J, Aboian M, et al. **High-grade neuroepithelial tumor with BCOR exon 15 internal tandem duplication: a comprehensive clinical, radiographic, pathologic, and genomic analysis.** *Brain Pathol* 2020;30:46–62 CrossRef Medline
13. Bremer J, Kottke R, Johann PD, et al. **A single supratentorial high-grade neuroepithelial tumor with two distinct BCOR mutations, exceptionally long complete remission and survival.** *Pediatr Blood Cancer* 2020;67:e28384 CrossRef Medline
14. Capper D, Jones DT, Sill M, et al. **DNA methylation-based classification of central nervous system tumours.** *Nature* 2018;555:469–74 CrossRef Medline

15. Astolfi A, Melchionda F, Perotti D, et al. **Whole transcriptome sequencing identifies BCOR internal tandem duplication as a common feature of clear cell sarcoma of the kidney.** *Oncotarget* 2015;6:40934–39 CrossRef Medline
16. Roy A, Kumar V, Zorman B, et al. **Recurrent internal tandem duplications of BCOR in clear cell sarcoma of the kidney.** *Nat Comm* 2015;6:8891 CrossRef Medline
17. Ueno-Yokohata H, Okita H, Nakasato K, et al. **Consistent in-frame internal tandem duplications of BCOR characterize clear cell sarcoma of the kidney.** *Nat Genet* 2015;47:861–63 CrossRef Medline
18. Kao YC, Sung YS, Zhang L, et al. **Recurrent BCOR internal tandem duplication and YWHAE-NUTM2B fusions in soft tissue undifferentiated round cell sarcoma of infancy: overlapping genetic features with clear cell sarcoma of kidney.** *Am J Surg Pathol* 2016;40:1009–20 CrossRef Medline
19. Santiago T, Clay MR, Allen SJ, et al. **Recurrent BCOR internal tandem duplication and BCOR or BCL6 expression distinguish primitive myxoid mesenchymal tumor of infancy from congenital infantile fibrosarcoma.** *Mod Pathol* 2018;31:374 CrossRef Medline
20. Dangouloff-Ros V, Tauziède-Espariat A, Roux CJ, et al. **CT and multimodal MR imaging features of embryonal tumors with multilayered rosettes in children.** *AJNR Am J Neuroradiol* 2019;40:732–36 Medline
21. Dangouloff-Ros V, Deroulers C, Foissac F, et al. **Arterial spin labeling to predict brain tumor grading in children: correlations between histopathologic vascular density and perfusion MR imaging.** *Radiology* 2016;281:553–66 CrossRef Medline
22. Jin B, Feng XY. **MRI features of atypical teratoid/rhabdoid tumors in children.** *Pediatr Radiol* 2013;43:1001–08 CrossRef Medline
23. Warmuth-Metz M, Bison B, Dannemann-Stern E, et al. **CT and MR imaging in atypical teratoid/rhabdoid tumors of the central nervous system.** *Neuroradiology* 2008;50:447–52 CrossRef Medline
24. Meyers SP, Khademian ZP, Biegel JA, et al. **Primary intracranial atypical teratoid/rhabdoid tumors of infancy and childhood: MRI features and patient outcomes.** *AJNR Am J Neuroradiol* 2006;27:962–71 Medline
25. Parmar H, Hawkins C, Bouffet E, et al. **Imaging findings in primary intracranial atypical teratoid/rhabdoid tumors.** *Pediatr Radiol* 2006;36:126–32 CrossRef Medline
26. Zuccoli G, Izzi G, Bacchini E, et al. **Central nervous system atypical teratoid/rhabdoid tumour of infancy. CT and MR findings.** *Clin Imaging* 1999;23:356–60 CrossRef Medline
27. Alrayahi J, Zapotocky M, Ramaswamy V, et al. **Pediatric brain tumor genetics: what radiologists need to know.** *Radiographics* 2018;38:2102–22 CrossRef Medline
28. Northcott PA, Korshunov A, Witt H, et al. **Medulloblastoma comprises four distinct molecular variants.** *J Clin Oncol* 2011;29:1408–14 CrossRef Medline
29. Mata-Mbemba D, Zapotcky M, Laughlin S, et al. **MRI characteristics of primary tumors and metastatic lesions in molecular subgroups of pediatric medulloblastoma: a single-center study.** *AJNR Am J Neuroradiol* 2018;39:949–55 CrossRef Medline
30. Yuh EL, Barkovich AJ, Gupta N. **Imaging of ependymomas: MRI and CT.** *Childs Nerv Syst* 2009;25:1203–13 CrossRef Medline